Light trimming of a narrow bandpass filter based on a photosensitive chalcogenide spacer

W. D. Shen,[1,2] M. Cathelinaud,[1] M. Lequime,[1*] F. Charpentier,[3] and V. Nazabal[3]

[1]*Institut FRESNEL, UMR CNRS 6133, Université Paul Cézanne – Ecole Centrale Marseille – Université de Provence Domaine Universitaire de Saint-Jérôme, 13397 Marseille Cedex 20, France*

[2]*Current address: State Key Laboratory of Modern Optical Instrumentation Zhejiang University, 310027 Hangzhou, China*

[3]*Sciences Chimiques de Rennes, UMR CNRS 6226, Université Rennes 1, 35042 Rennes, France*

*Corresponding author: michel.lequime@fresnel.fr

Abstract: We present an experimental study of the photosensitive properties of a narrow bandpass filter based on a $Ge_{15}Sb_{20}S_{65}$ spacer fabricated by electron beam deposition. For a single layer, near the optical bandgap of this chalcogenide material, the efficiency of the photo-bleaching increases as the central wavelength of the light source for exposure decreases. The maximum relative photo-induced change of the optical thickness reaches about 1%. By using controlled light exposure around 480 nm of a photosensitive narrow bandpass filter centered at 1550 nm, we obtained a spatially localized shift of its peak wavelength up to 5.4 nm. This property is used to perform, for the first time at our knowledge, the post trimming of a narrow bandpass filter with a light beam. A 5x5 mm^2 ultra uniform area in which the relative spatial variation of its peak wavelength remains below 0.004% is demonstrated.

©2008 Optical Society of America

OCIS codes: (310.6845) Thin film devices and applications; (310.6860) Thin films, optical properties; (160.5335) Photosensitive materials

References and links

1. C. C. Lee and K. Wu, "In situ sensitive optical monitoring with proper error compensation," Opt. Lett. **32**, 2118-2120 (2007).
2. M. Lequime and J. Lumeau, "Laser trimming of thin-film filters," Proc. SPIE **5963,** 60-69 (2005).
3. V. Nazabal, M. Cathelinaud, W. D. Shen, P. Nemec, F. Charpentier, H. Lhermite, M. L. Anne, J. Capoulade, F. Grasset, A. Moreac, S. Inoue, M. Frumar, J. L. Adam, M. Lequime, and C. Amra, "$Ge_{15}Sb_{20}S_{65}$ and $Te_{20}As_{30}Se_{50}$ chalcogenide coatings," Appl. Opt. **47**, C114-C123 (2008).
4. J. F. Viens, C. Meneghini, A. Villeneuve, T. V. Galstian, E. J. Knystautas, M. A. Duguay, K. A. Richardson, and T. Cardinal, "Fabrication and characterization of integrated optical waveguides in sulfide chalcogenide glasses," J. Lightwave Technol. **17**, 1184–1191 (1999).
5. A. M. Ljungstrom and T. M. Monro, "Light-Induced Self-Writing Effects in Bulk Chalcogenide Glass," J. Lightwave Technol. **20**, 78-85 (2002).
6. D. A. Turnbull, J. S. Sanghera, V. Nguyen, and I. D. Aggarwal, "Fabrication of waveguides in sputtered films of GeAsSe glass via photodarkening with above bandgap light," Mater. Lett. **58**, 51-54 (2004).
7. S. Ramachandran and S. G. Bishop, "Photoinduced integrated-optic devices in rapid thermally annealed chalcogenide glasses," IEEE J. Sel. Top. Quantum Electron. **11**, 260-270 (2005).
8. A. Saliminia, A. Villeneuve, T. V. Galstyan, S. LaRochelle, and K. Richardson, "First- and second-order Bragg gratings in single-mode planar waveguides of chalcogenide glasses," J. Lightwave Technol. **17**, 837-842 (1999)
9. M . Shokooh-Saremi, V. Taeed, I. Littler, D. Moss, B. Eggleton, Y. Ruan, and B. Luther-Davies, "Ultra-strong, well-apodised Bragg gratings in Chalcogenide rib waveguides," Electron. Lett. **41**, 13-14 (2005).
10. T. K. Sudoh, Y. Nakano, and K. Tada, "Wavelength trimming by external light irradiation-post-fabrication lasing wavelength adjustment for multiple-wavelength distributed-feedback laser arrays," IEEE J. Sel. Top. Quantum Electron. **3**, 577-583 (1997)
11. M. W. Lee, C. Grillet, C. L. C. Smith, D. J. Moss, B. J. Eggleton, D. F, B. Luther-Davies, S. Madden, A. Rode, Y. L. Ruan, and Y . H. Lee, "Photosensitive post tuning of chalcogenide photonic crystal waveguides," Opt. Express **15**, 1277-1285 (2007).

12. K. Tanaka, "Reversible photostructural change: Mechanisms, properties and applications," J. Non-Cryst. Solids **35-36**, 1023-1034 (1980)
13. S. R. Elliott, *Physics of Amorphous Materials* (Longman Scientific & Technical, Essex, 1990).
14. M. Frumar, J. Jedelsky, B. Frumarov, T. Wagner, and M. Hrdlicka, "Optically and thermally induced changes of structure, linear and non-linear optical properties of chalcogenides thin films," J. Non-Cryst. Solids **326-327**, 399-404 (2003).
15. M. Vlcek, M. Frumar, and A. Vidourek, "Photo-induced effects in Ge-Sb-S glasses and amorphous layers," J. Non-Cryst. Solids **90**, 513-516 (1987)
16. F. Lemarchand, C. Deumie, M. Zerrad, L. Abel-Tiberini, B. Bertussi, G. George, B. Lazarides, M. Cathelinaud, M. Lequime, and C. Amra, "Optical characterization of an unknown single layer: Institut Fresnel contribution to the Optical Interference Coatings 2004 Topical Meeting Measurement Problem," Appl. Opt. **45**, 1312-1318 (2006).
17. A. Zakery and S. R. Elliott, "Optical properties and applications of chalcogenide glasses: a review," J. Non-Cryst. Solids **330**, 1-12 (2003).
18. A. A. Othman, "Influence of ultraviolet irradiation on the optical properties of amorphous $Sb_{10}Se_{90}$ thin films," Thin Solid Films **515**, 1634-1639 (2006).
19. L. Abel-Tiberini, F. Lemarquis and M. Lequime, "Dedicated spectrophotometer for localized transmittance and reflectance measurements," Appl. Opt. **45**, 1386-1391(2006).
20. http://www.yokogawa.com/tm/pdf/comm/aq6315/buaq6315e.pdf
21. K. P. Chen, P.R. Herman, and R. Taylor, "Photosensitivity and Application with 157-nm F_2 Laser Radiation in Planar Lightwave Circuits," J. Lightwave Technol. **21**, 140-148 (2003).
22. H. A. Macleod, *Thin-Film Optical Filters,* 3rd Edition, (Institute of Physics Publishing, Philadelphia 2001).
23. M. Lequime, R. Parmentier, F. Lemarchand and C. Amra, "Toward tunable thin-film filters for wavelength division multiplexing applications," Appl. Opt. **41**, 3277-3284 (2002).
24. W. D. Shen, X. Liu, B.Q. Huang, Y. Zhu and P. F. Gu, "The effects of phase shift on the optical properties of a micro-opto-electro-mechanical system Fabry-Perot tunable filter," J. Opt. A-Pure. Appl. Op. **6**, 853-858 (2004).
25. J. Lumeau and M. Lequime, "Localized measurement of the optical thickness of a transparent window: application to the study of the photosensitivity of organic polymers," Appl. Opt. **45**, 6099-6105 (2006).
26. G. Pfeiffer, M. A. Paesler, and S. C. Agarwal, "Reversible photodarkening of amorphous arsenic chalcogens," J. Non-Cryst. Solids **130**, 111-143 (1991).

1. Introduction

Narrow bandpass filters (NBFs) are one of the key components in optics communications, fluorescence excitation/detection and laser-line cleaning. Today, as high energy deposition technologies like Ion Assisted Deposition (IAD) or Dual Ion Beam Sputtering (DIBS) develop, it became quite easy to manufacture most of the well-designed NBFs by optical monitoring with error compensation [1]. However, due to the high requirements on error tolerance and the limit of thickness uniformity in the deposition chamber, the production yield is still very low. Generally, there is only one circular ring on the whole substrate which will satisfy the final performance. Thus, the use of a photosensitive material for the spacer of NBFs [2] would be very attractive for enabling the post trimming of such devices with the help of a light beam. It could not only correct the consequences of some deposition errors on the filter properties accurately, but also create entirely new filtering devices with controlled spatial properties, for instance, variable filters with arbitrary profile or apodizing filter with spatially-structured transmission/reflectance response.

A chalcogenide glass of $Ge_{15}Sb_{20}S_{65}$ (2S1G) is compatible with optical thin film deposition process and presents high refractive index in the C-band associated to very low absorption and scattering levels [3]. At λ=1550 nm for instance, refractive index is equal to 2.4 and extinction coefficient is less than 10^{-4}. Therefore it can be used as high index material for the manufacturing of narrow bandpass filters in the near infrared region. Moreover, the photosensitivity of chalcogenide materials has been successfully utilized for the creation of directly written waveguides [4-7], strong Bragg gratings [8,9] and post-tuning of photonic crystal waveguides [10,11]. In this paper, we demonstrate a novel post-processing technique which utilizes the photosensitivity of chalcogenide material to modify the optical properties of thin film filters.

The content of this paper is organized as follows: the photosensitivity of 2S1G single layer is first studied in Section 2. Then we present in Section 3 the effect of a quasi monochromatic and spatially localized illumination on the optical properties of a narrow bandpass filter with a

photosensitive chalcogenide spacer. Section 4 is devoted to the first demonstration of the use of a light beam to perform the post trimming of such a filter and improve its uniformity on a 5x5 mm^2 area (final uniformity better than 4.10^{-5}). Finally, summary of the main achievements and further developments of this technique are given in Section 5.

2. Single 2S1G layer photosensitivity studies

The magnitude and sign of the photo-induced changes can be highly dependant on the chemical composition of chalcogenide material [12-14]. To identify the specific photosensitivity of 2S1G for which the origin of this phenomenon is not fully understood [15], a single layer of this material was first deposited on fused silica substrate by electron beam evaporation (Balzers BAK600). The deposition rate was 1 nm/second and the total thickness was about 630 nm as controlled by optical monitoring. Then this single layer was exposed for 2 hours in air with a Xenon arc lamp which emits high intensity radiation in a wavelength range between 400 nm and 1000 nm. The transmittance spectra of this single layer were measured before and after exposure from 480 nm to 1300 nm with a 1 nm interval.

After light exposure, the transmission curve [Fig. 1(a)] was slightly shifted toward shorter wavelengths. This effect reveals a photo-induced decrease of the optical thickness of the 2S1G film. It can be also seen that the transmittance in the short wavelength region was slightly increased after exposure. It indicates that the absorption was reduced. The optical constants, i.e., refractive index and extinction coefficient, were determined by the spectral curve fitting method with a global optimization algorithm [16]. The results of this determination are presented in Fig. 1(b) and Fig. 1(c). The refractive index (*n*) and extinction coefficient (*k*) in the whole spectral region are decreased. The changes are respectively Δn=-0.022 at 1.3 μm and Δk=-0.027 at 480 nm, with no obvious change of the film mechanical thickness. All these results are in accordance with a photo-bleaching effect usually observed for as-deposited films made of germanium based sulphide glasses [17].

(a)

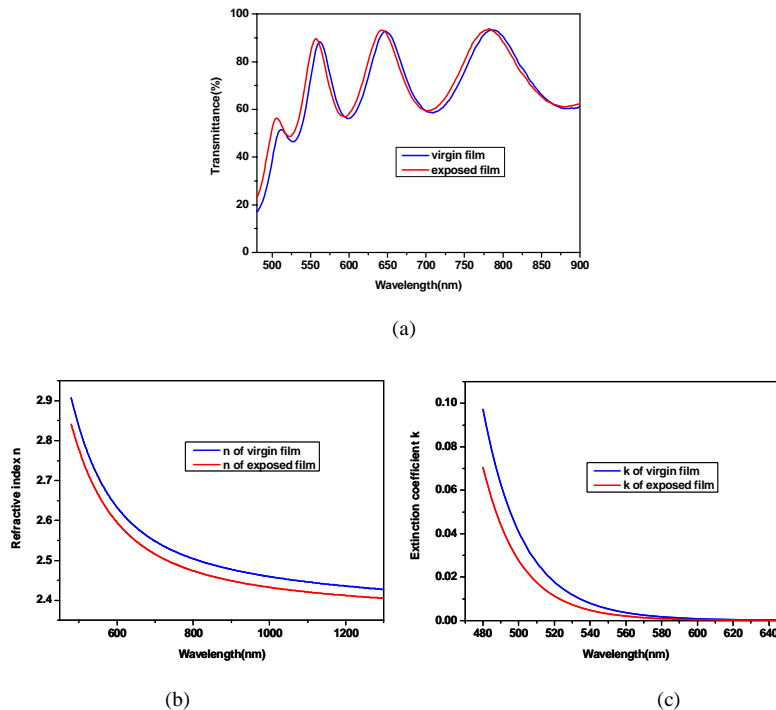(b)   (c)

Fig. 1. Influence of a broadband illumination on the optical properties of a 2S1G single layer. (a) Transmittance data. (b) Refractive index. (c) Extinction coefficient. The blue curves indicate the virgin film and the red curves the exposed film.

The photosensitivity of the chalcogenide is known to arise from structural rearrangements accompanying trapping of photo-excited carriers, and induced by the single photon absorption of light at frequencies near or below the optical bandgap of the material [17]. These subtle structural rearrangements lead to the change of refractive index. To a better understanding of this phenomenon on as-deposited $Ge_{15}Sb_{20}S_{65}$ film, we decided to investigate the effect of light exposure with various wavelengths on photosensitivity. The optical bandgap of the amorphous 2S1G can be determined from the absorption curve of the deposited film [18], which gives a value of 516.7 nm, i.e. about 2.4 eV.

A spectrophotometer previously developed in our team and which allows localized transmission and reflection measurements [19] was slightly modified to both expose the sample to a quasi monochromatic light beam with different wavelengths from 440 nm to 600 nm and perform an in situ measurement of the refractive index change induced by this exposure. The light source was a Xenon arc lamp. The quasi monochromatic light exposures were achieved by adding dedicated bandpass filters on the collimated light beam delivered by this light source. The central wavelengths of these bandpass filters were chosen in the spectral range of interest, i.e. 440, 460, 480, 500, 520, 540, 560, and 600 nm. The bandwidths of all these filters were around 10 nm, except at 600 nm where the bandwidth was about 40 nm. In order to avoid the possible exposure out of the interested band, the selected filters include metallic layer to achieve rejection level better than 0.1% from 300 nm to 3 μm. A neutral density filter with an optical density of 3.0 was added during the transmittance measurement to avoid a parasitic effect of the unfiltered light fluence. The selected NBFs and the neutral density filter were installed in a motorized filter wheel. Thus, the light with NBFs and neutral density filter were respectively used as the 'writing' beam and the 'probing' beam.

First of all, a small area on the sample (2 mm diameter) was selected and its spectral transmittance was measured from 500 nm to 1300 nm with the help of an Optical Spectrum Analyzer (OSA) ANDO AQ-6315A [20]: a real time determination of the optical thickness was performed by fitting the measured transmittance curve [16]. After selection of a first exposure wavelength, the corresponding bandpass filter was installed in the motorized wheel. The optical power density available at the sample surface was measured by the optical power meter function of OSA. Typical values were between 70 and 100 μW/cm^2 (except the case of 600 nm filter with a 0.45 mW/cm^2 density). Then, the sample was exposed for 30 minutes and spectral transmittance was measured again, providing an updated version of the optical thickness. These three actions (monochromatic light exposure, transmittance measurement, and optical thickness determination) were finally repeated for 60 times. By using the result of the optical power density measurement, we were able to transform the accumulated exposure time into accumulated fluence, and to draw the variations of the optical thickness @ 750 nm with respect to the accumulated fluence of the 'writing' beam. Note that this method is mainly sensitive to an optical thickness change and it is here difficult to distinguish a small variation of refractive index (*n*) of thin film from a small variation of its physical thickness (*d*).
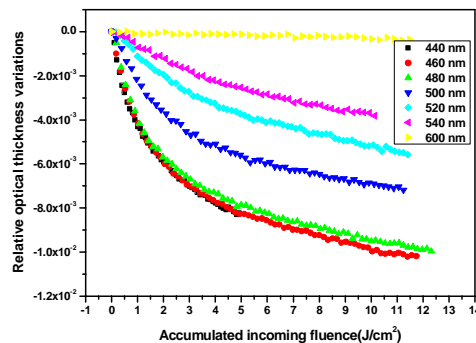

Fig. 2. Relative optical thickness variations versus the accumulated incoming fluence at different wavelengths around the optical gap of the chalcogenide 2S1G material (516.7 nm)

This study was repeated for all the exposure wavelengths previously listed by selecting a new zone at the sample surface for each new wavelength. The whole results are combined in Fig. 2. It can be seen in all these curves that the optical thickness quickly decreases at first as the accumulated fluence increases and gradually saturates. Moreover, the response of the photo-induced change turns quicker and larger as the exposure wavelength decreases. The optical thickness variation is very small at 600 nm, an exposure wavelength which is relatively far away from the optical bandgap of 2S1G (516.7 nm).

For each wavelength, the optical thickness change can be described by the following classical relationship:

$$\Delta(nd) = \Delta(nd)_0 \left[1 - e^{-F/F_0}\right] \tag{1}$$

where $\Delta(nd)$ is the optical thickness change for a fluence F (in J/cm^2), $\Delta(nd)_0$ is the maximum optical thickness change (saturated value), and F_0 is a characteristic fluence describing the sensitivity of the material at this wavelength. Figure 3 shows an example of the very good agreement between the experimental data (here @ 500 nm) and such a modeling.
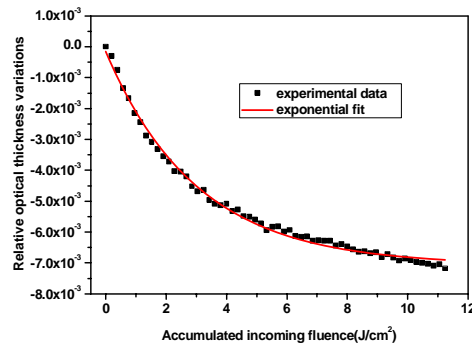

Fig. 3. Illustration of the agreement between the recorded data and the modeling defined by Eq. (1)

These last two quantities [$\Delta(nd)_0$ and F_0] are obviously wavelength dependent and one can see in Fig. 4 the variation of the absolute value of the saturated relative photo-induced optical thickness change $|\Delta(nd)_0|/(nd)_0$ with respect to the wavelength of exposure. This quantity increases as the exposure wavelength decreases. The results agree with that of a germanosilicate glass [21]. However, the variation of $|\Delta(nd)_0|/(nd)_0$ values are very small when exposure wavelengths are less than 480nm. We can explain this effect by investigating the electrical field intensity distribution inside the single layer which determines the effective light fluence of exposure.
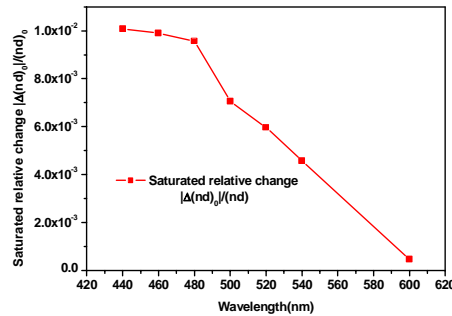

Fig. 4. Spectral dependence of the saturated relative change $|\Delta(nd)_0|/(nd)_0$ of the optical thickness of 2S1G single layer

By the classical matrix method [22], the electrical field intensity distribution inside the layer is simulated. Figure 5(a) shows the results at 460 nm, 520 nm and 600 nm which are normalized by the incoming intensity in air medium. We observe that the standing wave forms inside the layer at λ=600 nm because of the interference between the transmitted and reflected wave. At λ=520 nm near the optical bandgap of the material, a standing wave with slowly attenuated magnitude can also be seen. However, due to the high absorption of 2S1G at 460 nm, this standing wave disappears and the electrical field intensity attenuates rapidly until zero inside the layer. It indicates that only a part of the film could be exposed and could produce the photo-induced change at this wavelength of exposure. The extinction coefficient of 2S1G increases quickly in short wavelength region as shown in Fig. 1(c). Thus the depth of light penetration decreases as the wavelength decreases. The exposed thickness will be also reduced though the corresponding photon energy increases at short wavelength. Therefore, the total photo-induced change inside the whole layer will be very similar. It is the reason why there is a small difference of $\Delta(nd)_0$ values when the exposure wavelength is less than 480nm.
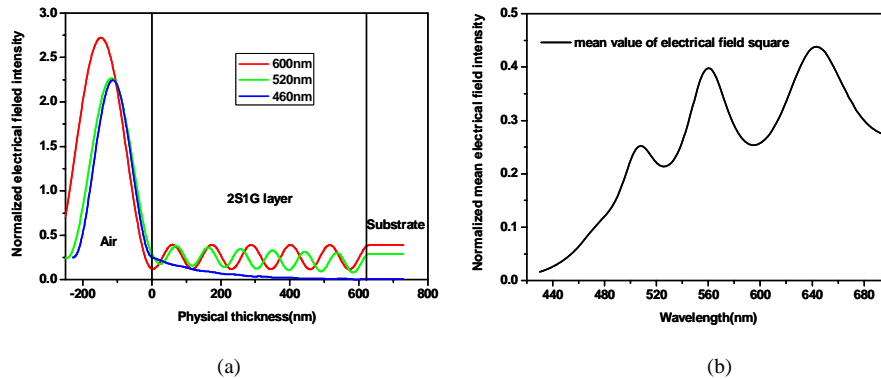
Fig. 5. (a). Electric field intensity distributions inside the layer normalized by the intensity of the incoming beam (Red curve 600nm, green curve 520nm and blue curve 460nm). (b) Spectral dependence of the ratio between the mean values of the square electrical field inside the film and that of the incoming beam.

Because of the interference effect induced by the air/2S1G and 2S1G/substrate interfaces and the absorption of 2S1G, the effective exposure fluence is not the optical power density measured at the sample surface during the experiment, but proportional to the mean electrical field intensity inside the layer. Spectral dependence of the ratio between the mean values of the square electrical field and the intensity of the incoming beam is simulated and displayed in Fig. 5 (b). It is then possible to transform each characteristic fluence F_0 into a new one, called **effective** characteristic fluence and noted E_0, by using this ratio as a multiplicative corrective factor.
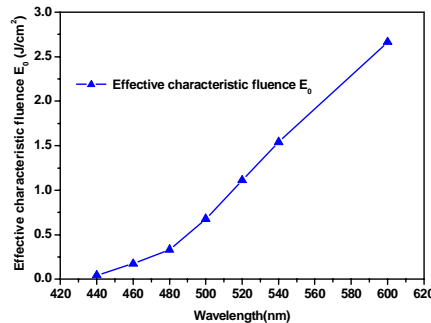
Fig. 6. Spectral dependence of the 2S1G effective characteristic fluence E_0

The variation of this effective characteristic fluence E_0 with respect to the wavelength of exposure is shown in Fig. 6. E_0 increases monotonously with the wavelength. It means that the speed of photosensitive response is quicker at the short wavelength exposure than the long wavelength one because of the higher photon energies.

3. Photo-induced changes of a narrow bandpass filter with 2S1G spacer

3.1 Manufacturing and charactering of the narrow bandpass filter

Narrow bandpass filters $(HL)^4 6P (LH)^4$ using 2S1G material as a photosensitive spacer were manufactured by electron beam evaporation where H, L and P are respectively a quarterwave of zinc sulfide (ZnS), cryolite (Na_3AlF_6) and 2S1G at $\lambda_0=1550$ nm. During the deposition of the filter, the optical monitoring with turning point method [3] was used to control the thickness of each layer. After manufacturing, the transmittance was measured using our dedicated spectrophotometer (see Fig. 7). The peak wavelength, the bandwidth, and the maximum transmittance are 1546.5 nm, 4 nm and 72.8% respectively. ZnS (n=2.25) and Na_3AlF_6 (n=1.3) were chosen because of their good compatibility with 2S1G. We also investigated the use of oxides, respectively silica (SiO_2) and tantala (Ta_2O_5), for the manufacturing of low and high index layers of the dielectric mirrors $(HL)^n$, but the long-term mechanical behavior of the filters including a 2S1G spacer was not satisfactory (cracks appearance).
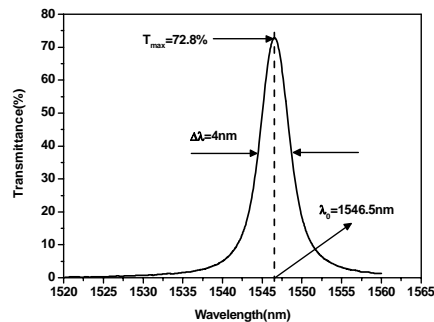

Fig. 7. Spectral transmittance of a narrow bandpass filter with photosensitive chalcogenide spacer

3.2 Choice of the trimming wavelength

The electrical field intensity inside the photosensitive layer directly determines the effective exposure fluence and the consequent photo-induced change. Thus, after exposure, the photo-induced refractive index change inside the spacer of NBF will be sine modulated which is similar to that of the single layer shown in Fig. 5(a). Additional simulations show that such a modulation has no obvious effect on the shape of the spectral profile of NBF except a shift of the peak wavelength [2]. This shift is dependent on the mean value of the refractive index change inside the spacer. The key parameter for evaluating the efficiency of a NBF trimming is then the normalized mean electrical field intensity inside the spacer layer.

The mean value inside the spacer layer of our NBF at each wavelength in the interested spectrum (from 430 nm to 620 nm) is calculated and displayed in Fig. 8. The effective intensity of electric field was greatly reduced compared with its value for the incoming light. In the rejection band of dielectric mirror from 500 nm to 570 nm, the intensity is very small except a peak near 550 nm which is the high order resonant wavelength. In the spectral range comprised between 430 nm and 490 nm, due to the increase of absorption, the mean electrical field intensity decreases gradually as the wavelength decreases.

By combining these modeling results with the results of photosensitivity dependence on the exposure wavelength previously obtained in a single layer (see Fig. 6), we can predict the

effect of a light exposure with different wavelengths on the photo-induced change of the NBF spacer. The most efficient wavelength for trimming our filter is near 490 nm. So the quasi monochromatic light obtained from the 480 nm bandpass filter will be used to expose our photosensitive filter.
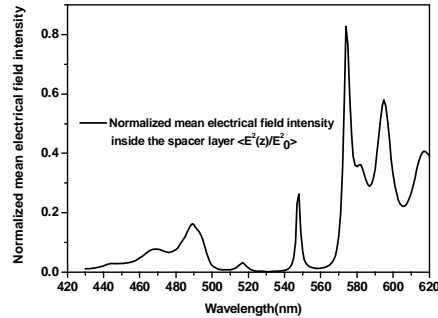

Fig. 8. Normalized mean electrical field intensity inside the NBF spacer layer in the 430-620 nm wavelength range

3.3 Photo-induced change of NBF

The transmittance of NBF was measured in situ every 30 minutes during a 480 nm exposure. Figure 9(a) shows the recorded spectrum at different exposure times. The transmittance curve was observed to shift gradually towards shorter wavelength with increasing exposure. It indicates a negative photo-induced index change which is in accordance with the results previously obtained on the single 2S1G material. There is no obvious variation of the peak transmittance T_{max}. Figure 9(b) shows a plot of the peak wavelength versus exposure time. The resonant wavelength shifts quickly at first but displays saturation behavior at longer time. The maximum wavelength shift was here 5.4 nm.
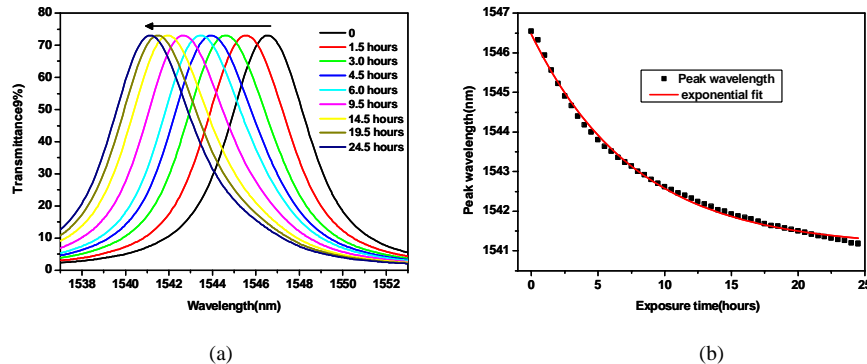

(a)

(b)

Fig. 9. (a). Measured NBF transmittance curves for different accumulated time of exposure at 480 nm. (b) Shift of the peak wavelength versus accumulated exposure time

The curve could be well fitted by the same exponential Eq. (1) as used for the modeling of the optical thickness change. To achieve an appropriate comparison between these data and the experimental results obtained on a single layer, numerous computations have to be performed.

First, we have to transform the duration of the exposure at 480 nm into the effective accumulated fluence E inside the spacer of NBFs: it can be easily achieved by combining the result of the power density measurement performed in front of the sample at this specific wavelength, the duration of the exposure, and the normalized mean electrical field intensity. Then this effective accumulated fluence E has to be used to estimate the relative optical

thickness change $\Delta(nd)/(n_0d_0)$ in the spacer layer of the NBF based on the measured results of the single layer.

Finally this ratio has to be converted into a relative peak wavelength shift of the NBF, which can be achieved by applying the following relation [23]:

$$\frac{\Delta\lambda_0}{\lambda_0} = \kappa\frac{\Delta(nd)}{nd} \tag{2}$$

where κ is a positive coefficient, typically between 0.3 and 1, and whose exact value is connected to the structure of the NBF high reflection mirrors [24]. In our structure, κ is equal to 0.7049. Figure 10 shows the final result of this comparison between the measured shifts of Fig. 9(b) and the results deduced from the photo-induced change of a single 2S1G layer.
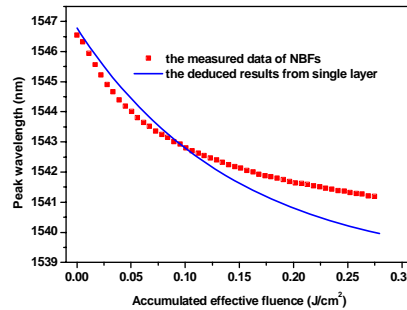

Fig. 10. Comparison of the NBF peak wavelength shifts with 480nm light exposure between the measured results and the deduced values from single layer photo-induced change.

The agreement is satisfactory, even if we can observe some differences between the two curves that directly result from the deposition error. Indeed, the manufactured NBF is not perfectly identical to the designed one. Thus, the asymmetry of two mirrors in NBF will induce some variations of the κ term in Eq. (2). Moreover, the simulated value of electrical field intensity will differ from the actual one, especially at the exposure wavelength (480 nm) which is far away from the monitoring wavelength of turning point method (1545 nm).

After the exposure, a mapping of the exposed area of NBF was carried out with a small beam size (400 μm) on a dedicated mapping bench developed in our team and which uses a tunable laser instead of an optical spectrum analyzer [25]. Figure 11 shows the peak wavelength distribution recorded in an 8x8 mm^2 area. A valley could be clearly observed and the peak wavelength change almost perfectly reproduces the shape of the exposure beam.
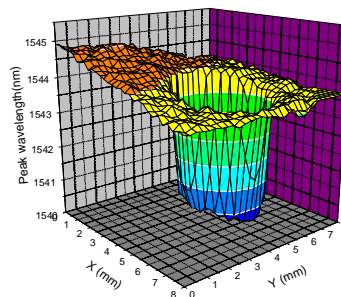

Fig. 11. Spatial variations of the NBF central wavelength after the 480 nm exposure

4. Light trimming of a narrow bandpass filter

Based on the above results on the photo-induced changes of our chalcogenide spacer NBF, we can now try to spatially trim the central wavelength of such a filter, point by point, in order to obtain a narrow bandpass filter with ultra-uniform spatial properties. Because of the relative low illumination level provided by the Xenon arc lamp, when exposed around 480 nm, this trimming process can be very long and ineffective. In the future, it can be clearly advantageous to replace this filtered lamp by an argon laser line. However, to increase the trimming speed by keeping the same bench as used during all this study, we decided to use the same Xenon arc lamp but unfiltered to expose the filter. With such operating conditions, a maximum shift of 6.3 nm in the peak wavelength can be achieved for a 280 minutes exposure. It is much quicker than the quasi monochromatic exposure.

The trimmed area was 5x5 mm^2. A 1 mm light beam was used to trim the filter with a spatial resolution of 1 mm. The total number of trimmed points was then 25. The mapping of the peak wavelength distribution before trimming is displayed in Fig. 12(a). It can be seen that the maximum variation of the NBF peak wavelength was about 3 nm.
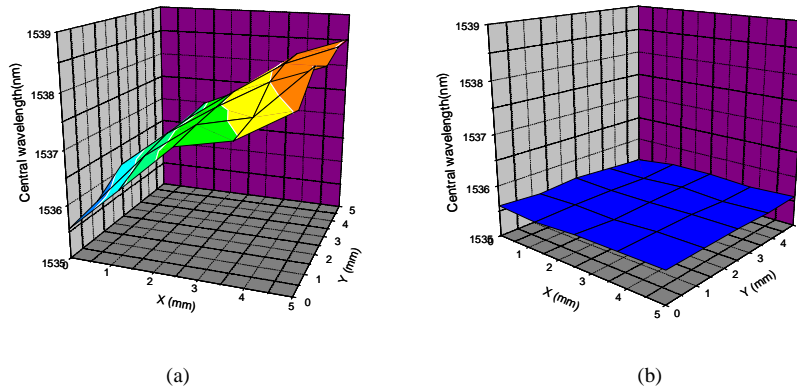

(a)   (b)

Fig. 12. Mapping of the peak wavelength distribution in a 5x5 mm^2 area: (a) before trimming (b) after trimming

Due to the nature of the photosensitivity of the 2S1G (photobleaching effect associated to negative refractive index change), the minimum peak wavelength over the whole area was chosen as the target value. For each point, the needed exposure time (T) was calculated using relationship between the peak wavelength shift and the exposure time with full band exposure. Then, to trim the filter very accurately, we carried out a multi-step exposure. The transmittance and peak wavelength were measured after 60% of the T exposure time. Then, the left exposure time was determined and exposure was resumed until reaching 60% of remaining time. Finally this procedure will be repeated until the peak wavelength reaches the target value. In general, 3 or 4 loops are required. In our case, after about 10 hours, the trimming process of the whole area was finished. Figure 12(b) shows the peak wavelength distribution in the processed area after trimming. The maximum peak wavelength difference in this area is 0.05nm and the relative uniformity is therefore 3.2x10^{-5}.

The long term stability of the filter's optical properties is very important for application. To investigate the stability of a filter with chalcogenide spacer, the transmittance of such a filter at the trimmed area was measured automatically every 4 hours on our dedicated setup where a temperature controller with 0.02^{0}C accuracy was used to hold the sample [25]. This measurement was performed in a black room in order to avoid possible background light influence. Figure 13 shows the peak wavelength variations for 12 days duration. The maximum change was ±0.05 nm, with no drift evidence. This variation maybe results from a lack of repeatability in the positioning of the sample with respect to the probing beam, or from

moisture absorption effects, but remains compatible with our uniformity target for a first demonstration of this light processing scheme.
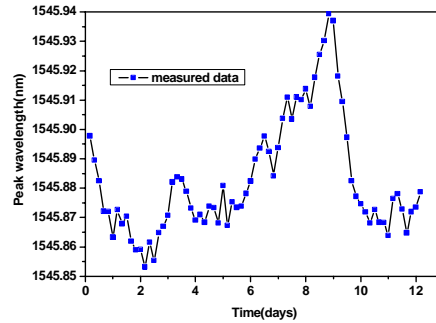

Fig. 13. NBF peak wavelength variations at the trimmed area for 12 days duration (every point indicates 4 hours).

The long-term stability of the trimmed filter is directly connected to the irreversibility of the refractive index changes induced by the light exposure. Our results are in accordance with the behavior of un-annealed amorphous arsenic chalcogens thin films prepared by vacuum deposition [26]. Reversible changes are more usually observed in well-annealed thin films or melt quenched bulk glasses.

Another important item in relation with long-term stability is to avoid spontaneous change of the filter properties induced by its use: it means first that, after trimming, this filter could be used only in a spectral region far away from the optical gap of photosensitive material, for instance the C-band of the optical telecommunication range. But it can also require preventing a possible illumination of the spacer by a visible light beam, mainly from the environment like sunshine, daylight lamp, etc. It can be easily obtained by adding to the processed filter some colored glasses having a high absorbance in the entire visible spectrum.

5. Conclusion

In conclusion, we presented the first experimental demonstration of light trimming of NBFs based on photosensitive material. For single $Ge_{15}Sb_{20}S_{65}$ layer, we studied the photosensitivity dependence on the exposure spectrum near the optical bandgap. It indicates that the maximum photo-induced change of optical thickness increases as the exposure wavelength decreases. Then, narrow bandpass filters with 2S1G spacer were manufactured. 480 nm light exposure resulted in a 5.4 nm shift in peak wavelength towards the shorter wavelength. Using these results, a first prototype of ultra-uniform NBFs in 5x5 mm^2 area was fabricated by spatial trimming of the individual component. A relative uniformity of $3.2x10^{-5}$ was obtained. Long term stability of this filter was finally demonstrated.

The photosensitive response of NBF exposed by an argon laser line will be studied in the future and it is expected to reduce the trimming time greatly. This post-processing technique is highly promising for thin film filter manufacturing either to correct the deposition error or create new spatially-structured filters.

Acknowledgment